

# Influence of talc morphology on the mechanical properties of talc filled polypropylene

Luciana A. Castillo · Silvia E. Barbosa · Numa J. Capiati

Received: 18 December 2012 / Accepted: 17 April 2013 / Published online: 30 April 2013  
© Springer Science+Business Media Dordrecht 2013

**Abstract** Injected polypropylene (PP)/talc composites were studied to evaluate the influence of different talc morphologies on their final mechanical properties. Talc genesis is responsible for type and content of associated minerals, crystalline degree, particle size distribution, and specially, morphology. Consequently, when talc is incorporated into PP, differences in the genesis mean differences in particle morphology and may influence the composite properties. Two talc samples having predominant macro and microcrystalline morphologies were used to prepare two composite sets to be tested. Thermal and mechanical properties of each PP/talc composites set were measured, analyzed and discussed comparatively. The results reveal that the main influences of talc morphology are given on modulus, yield strength and elongation at break of PP/talc composites. Macrocrystalline morphology of talc induces better composite mechanical properties than microcrystalline one. This behavior could be explained by talc characteristics as lamellarity, crystalline character and crystallinity degree.

**Keywords** Mechanical properties · Talc morphology · Polypropylene · Composites

## Introduction

In recent years, particulate-filled polymer composites have acquired significant technological importance. Fillers incorporation into thermoplastics is a common practice in plastic industry. At the beginning, they were used mainly to reduce

the production costs, but later fillers proved to be effective to enhance the polymer properties as well. These composites have been used for many new applications due to their low cost, easy processability and isotropic properties. Another important feature of particulate composites is their suitability to fit in a specific application, favored by their ability to tailor final properties by changing processing variables [1].

Mineral fillers affect the final mechanical properties of thermoplastic matrix in two ways: by their inherent characteristics and by inducing changes in crystal morphology of the polymer matrix. In the last case, variations in the matrix crystallinity can modify the bulk properties of the composite. Furthermore, filler morphology, crystalline degree, particle size (average and distribution), and aspect ratio have a significant influence on the performance of polymer composites. Particularly, mineral filled PP has achieved great interest in both research and industrial field due to it is well known that PP exhibits good processability and accepts a broad range of natural and synthetic fillers [1].

Talc is one of the most common filler to reinforce PP because of its low cost and the convenient platy particle morphology. It is a naturally occurring magnesium silicate with an ideal chemical formula of  $Mg_3Si_4O_{10}(OH)_2$ . Due to the variety of ways in which the geological formation of talc occurred, every talc deposit is unique with regards to both chemistry and morphology [2]. According to the genesis, the size of individual talc platelets (a few thousand elementary sheets) can vary from approximately 1  $\mu m$  to over 100  $\mu m$  [3]. Talc morphology depends on its lamellarity which is determined by the individual platelet size. Different talc morphologies are distinguished, ranging from long, well-defined and stacked up platelets ('macrocrystalline' type, high lamellarity) to a heterogeneous stack of small and irregular platelets ('microcrystalline' type, low lamellarity). In this sense, macrocrystalline talc has large individual platelets (50–200  $\mu m$ ), higher aspect ratio, higher crystallinity, lower

L. A. Castillo · S. E. Barbosa (✉) · N. J. Capiati  
Planta Piloto de Ingeniería Química (UNS - CONICET), Camino  
La Carrindanga Km. 7,  
8000 Bahía Blanca, Argentina  
e-mail: sbarbosa@plapiqui.edu.ar

specific surface area ( $<10 \text{ m}^2/\text{g}$ ), and their particles are difficult to be micronized. On the other hand, microcrystalline talc has small irregular platelets ( $\sim 10 \text{ }\mu\text{m}$ ), lower crystallinity and is easily milled to very fine products of higher specific surface area ( $10\text{--}20 \text{ m}^2/\text{g}$ ). In addition, new mineral phases could be created from preexisting ones during the geological talc formation. As a consequence, ores are constituted by associated minerals mixtures, including mainly magnesite ( $\text{MgCO}_3$ ), calcite ( $\text{CaCO}_3$ ), dolomite ( $\text{CaMg}(\text{CO}_3)_2$ ) and chlorites ( $\text{Mg}_5(\text{Al,Fe})(\text{Al,Si})_4\text{O}_{10}(\text{OH})_8$ ) in a lesser proportion [2]. In this sense, chemical and structural parameters of any talc sample are indicative of its origin and crystallization conditions. For this reason, talc ores differ in chemical composition, morphology, associated minerals amount, whiteness and other properties.

In our group, a low-cost surface modification of talc was proposed [4]. This treatment is based on the reaction between acetic acid and talc, allowing the grafting of acetoxy groups ( $-\text{OCOCH}_3$ ) onto the particle surface and rendering talc more compatible with PP. These modified talc particles have an improved dispersion and distribution within PP matrix and an enhanced interfacial adhesion with PP. Mechanical properties of these composites were found to improve respect to PP-untreated talc ones, especially the tensile strength and the elongation at break [5]. However, the effect of filler morphology on composite mechanical properties has not been previously considered. In this work, the influence of talc morphology in PP/talc composites is studied by using two talc samples from different ores with different geological characteristics. A comparative analysis of composite thermal and mechanical properties is performed and the results are related to morphological talc characteristics taking into account their lamellarity, crystalline character and crystalline degree.

## Experimental section

### Materials

Commercial PP was used as polymer matrix (Melt Flow Index:  $1.8 \text{ g}/10 \text{ min}$ ,  $M_w$ :  $303,000 \text{ g/mol}$ ,  $M_w/M_n$ :  $4.45$ ), supplied by Petroquímica Cuyo. In order to improve the compounding with talc particles, PP pellets were reduced by a plastic grinder mill obtaining particles with an average length of  $1,700 \text{ }\mu\text{m}$ . Two talc samples from different geological genesis were used in the present study: Australian talc (A10) with a purity degree of  $98 \%$ , and Argentinean talc (SJ10) containing up to  $15 \text{ wt.}\%$  of associated minerals. These materials were supplied by Dolomita S.A.I.C. Both samples have similar average particle size ( $d_{50}=4.53\pm 1.65$  and  $d_{50}=5.86\pm 3.59 \text{ }\mu\text{m}$ , respectively). Main differences in morphological features between A10 and SJ10 samples can

be appreciated from the scanning electron microscopy (SEM) images in Fig. 1. These micrographs were taken in a Jeol 35 CF microscope on gold coated specimens. Figure 1a shows typical particles of microcrystalline talc in A10 sample, consisting of rounded and pseudo-spherical shape of particle aggregates where small particles are curved due to their elasticity and having face to face links between them. By grinding, these aggregates are separated and reduced to individual small particles which retain their tendency to curve. On the other hand, SJ10 particles appear as blocks having flatter and thicker cleaved particles with abrupt and well defined borders (Fig. 1b), being characteristic aspects of macrocrystalline talc. Figure 2 shows X-ray diffractograms of each talc sample and PP. They were carried out in a PW1710 BASED diffractometer at  $45 \text{ kV}$  and  $30 \text{ mA}$ , CuK and monocromator. The  $2\theta$  values ranged from  $2$  to  $60^\circ$ . Talc morphology can be characterized by the morphology index (MI) which is related to the intensity of (004) and (020) XRD peaks [6]. The MI index can vary from  $0$  for  $100 \%$  microcrystalline samples to  $1$  for  $100 \%$  macrocrystalline ones. For example, McCarthy et al. [7] found that MI index varied from  $0.98$  for the highly macrocrystalline and platy Vermont talc to  $0.45$  for the microcrystalline Montana ore. In the present study, MI is  $0.45$  for A10, and  $0.83$  for SJ10; confirming the predominant micro and macrocrystalline morphology observed in Fig. 1, respectively. From XRD spectra in Fig. 2a, the presence of associated minerals in each sample can be observed. On the other hand, the main PP reflections in Fig. 2b correspond to  $\alpha$  monoclinic crystalline phase: (110), (040), (130), (111) and (041) planes and  $\beta$  hexagonal crystalline phase, (300) plane. The discussion of the characterization described above was included in a previous paper [4].

### Composites processing and characterization

PP/talc composites were blended by melt extrusion in a Goettfert counter-rotating twin screw extruder ( $D=30 \text{ mm}$ ,  $L/D=25$ ) with a cylindrical die ( $1 \text{ mm}$ ) and a screw velocity of  $30 \text{ rpm}$ . Barrel temperature profile from hopper to die was  $170 \text{ }^\circ\text{C}$ – $190 \text{ }^\circ\text{C}$ – $200 \text{ }^\circ\text{C}$ – $210 \text{ }^\circ\text{C}$ – $220 \text{ }^\circ\text{C}$  and it was hold constant during composite blending. After extrusion, composite was solidified by passing it through a water bath and finally pelletized. PP/talc composites were prepared with concentrations of  $1$ ,  $3$ ,  $5$  and  $10 \%$  w/w and were named as *PP(Talc concentration)(Type of talc)*. Tensile test specimens were prepared on a Fluidmec 60 T injection-molding machine ( $D=40 \text{ mm}$ ,  $L/D=19$ ), according to ASTM D638. The temperature profile from hopper to nozzle was  $165 \text{ }^\circ\text{C}$ – $190 \text{ }^\circ\text{C}$ – $195 \text{ }^\circ\text{C}$ – $210 \text{ }^\circ\text{C}$ .

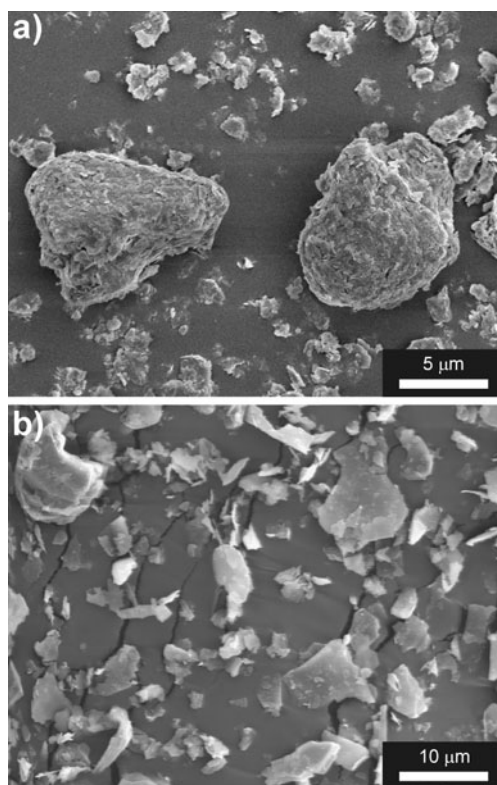


**Fig. 1** SEM micrographs of talc samples **a** A10 and **b** SJ10

Blend morphology as well as talc dispersion and distribution were studied by SEM on several points of cryofractured and gold coated surfaces of composite samples.

Thermal behavior of PP and PP/talc composites were assessed by Differential Scanning Calorimetry (DSC) under dynamic conditions using a Perkin Elmer Pyris 1 DSC. Tests were carried out in nitrogen atmosphere at a heating/cooling rate of 10 °C/min, between 30 and 220 °C. After the first heating step, each sample was left in the molten state for 1 min to erase the thermal history, previous to the crystallization step. Then, a second heating step was run. The matrix crystallinity degree ( $X_c\%$ ) was calculated from the melting enthalpy ratio of the composite and the corresponding to 100 % crystalline PP (209 J/g), making corrections in order to take into account the real amount of polymer in the composite.

Possible thermo-oxidative degradation induced by composite blending as well as the actual talc concentration in all composites was assessed by Fourier Transform Infrared Spectroscopy (FTIR) in a Thermo Nicolet Nexus FTIR spectrometer. Composite films of  $170 \pm 10 \mu\text{m}$  thickness were tested with a resolution of  $4 \text{ cm}^{-1}$  and integrating 10 scans. Thermo-oxidative degradation was estimated semi quantitatively by the carbonyl index, defined as the ratio of the areas under the band assigned to carbonyl group ( $1,700\text{--}1,800 \text{ cm}^{-1}$ ) and a reference band corresponding to PP, which is

not affected by the degradation ( $2,720 \text{ cm}^{-1}$ ). On the other hand, talc concentration was assessed by comparing the same PP band with a characteristic talc one ( $670 \text{ cm}^{-1}$ ). Previously, a calibration curve was done by using well known talc concentration composites.

Crystalline phases, crystal orientation and crystallinity degree of all prepared composites were analyzed by XRD. The spectra were taken directly on the surface of injected specimens in order to analyze the induced phases during processing.

Tensile mechanical properties were measured at room temperature in an Instron universal testing machine (Model 3369) with a strain rate of 70 mm/min up to sample breakage, following ASTM D638-03 test procedure. Young modulus, yield stress and elongation at break were determined, testing at least ten samples for each composite and reporting the average values.

## Results and discussion

### Composites structure analysis

As it is well known, performance of particulate composites besides filler characteristics is determined by particle dispersion and distribution within the matrix. Particle dispersion must be good enough to prevent the creation of stress-concentration sites that could start from agglomerated particles. Also, a smooth particle distribution contributes to uniform composite properties. Talc dispersion and distribution within PP matrix are analyzed by SEM on cryogenically fractured surface of composites, as it is seen in Fig. 3. Proper talc dispersion is observed at different points of the sample cross sections. Filler does not show agglomeration, even for 10 wt.% talc. Also, a preferred orientation of talc particles is appreciated for both set of composites, resulting from their platelike structure and their motion in a viscous medium during the compounding process. A comparative examination between fractured surfaces of PP/A10 and PP/SJ10 composites (especially at 10 wt.%) shows differences in particle size between talc samples. These can be attributed to the particle morphology and the possible disaggregation during compounding. A10 talc has microcrystalline morphology with large rounded aggregates constituted by thin laminar particles. These aggregates are opened during compounding in the twin screw extruder, either due to particle-particle attrition or high shear fields; resulting in smaller and irregular particles which are well distributed and dispersed for all concentrations. In the case of SJ10 talc, particle disaggregation is less evident as each particle is formed by flatter stacked layers. Although the dispersion and distribution in PP/SJ10 composites is good, talc particles are larger and thicker than that in PP/A10 composites.

**Fig. 2** XRD spectra of **a** A10, SJ10 and **b** PP. Ref: *T* talc, *Ch* chlorite, *C* calcite, *D* dolomite, *Mg* magnesite

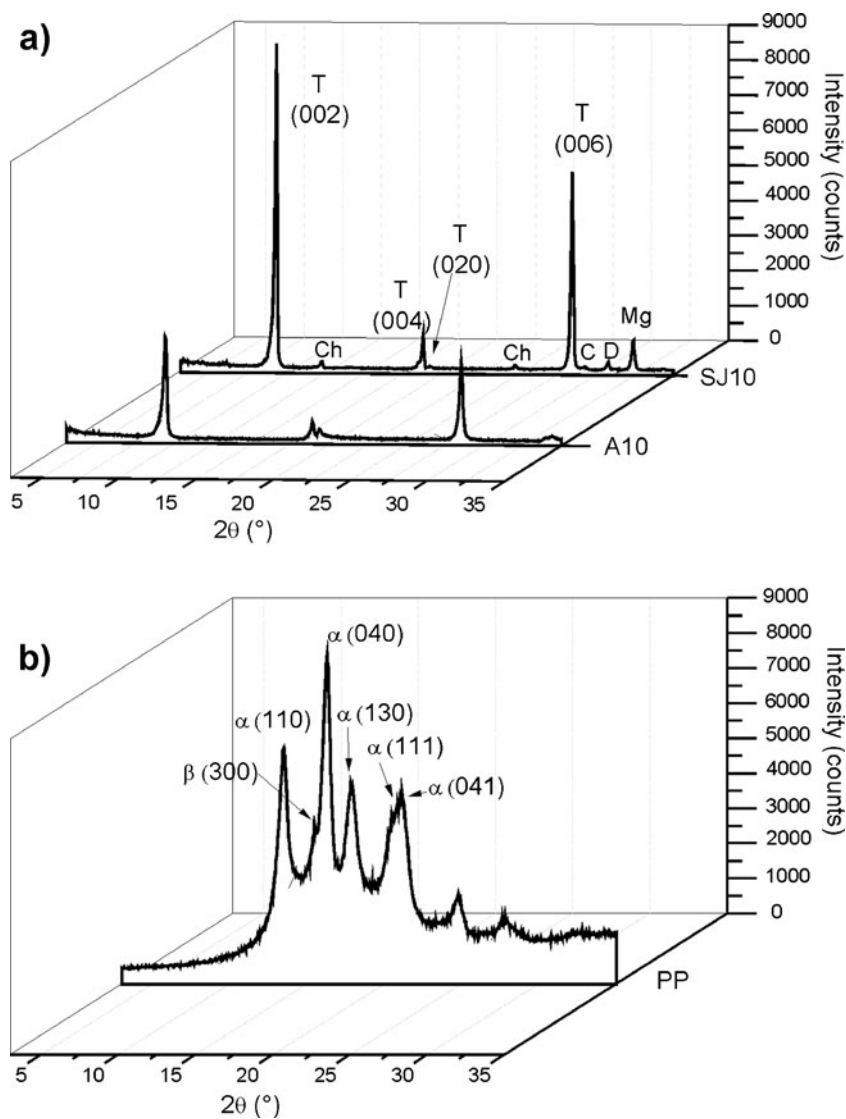
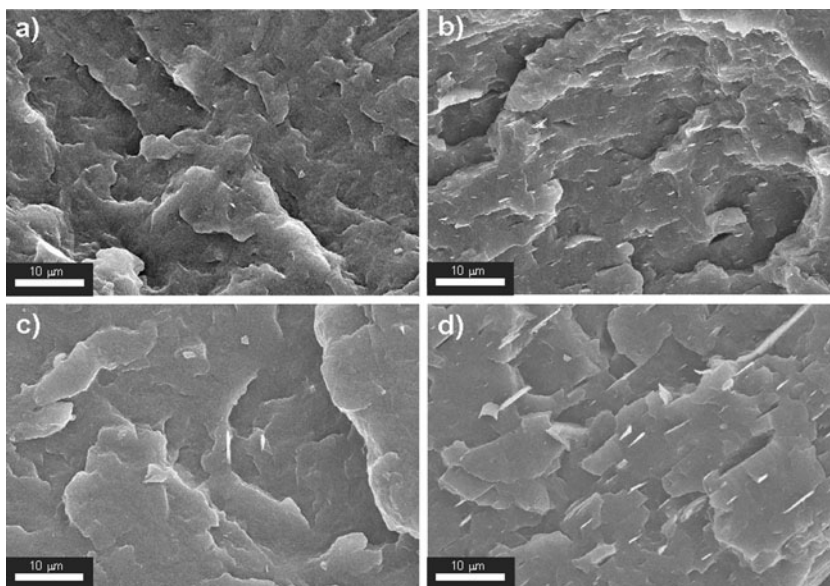


**Fig. 3** SEM micrographs (5000 $\times$ ) of composites **a** PP1A10, **b** PP10A10, **c** PP1SJ10 and **d** PP10SJ10





During composite compounding, molten material is exposed to high temperatures and shear fields which could cause thermo-oxidative degradation with consequent molecular weight and mechanical properties detriment. In order to detect possible thermo-oxidative degradation, carbonyl band was followed by FTIR for all the composites. Figure 4 shows the spectra of pure PP, PP/A10 and PP/SJ10 composites with 1 and 10 % wt of talc. Carbonyl index is less than 0.55 either for PP or PP/talc composites, being lower than the needed to trigger degradation, as it was reported in literature for the same materials and processing conditions [8].

Particle dispersion and distribution within the matrix, after composite compounding and injection molding, could be also estimated from the actual talc concentration. FTIR was used to determine this concentration through the ratio of talc ( $670\text{ cm}^{-1}$ ) to PP ( $2,720\text{ cm}^{-1}$ ) bands at different sections of the specimens. Bands ratio was calculated and compared to the values of a calibration curve. For all the composites, nominal talc concentration was very close to actual one. In addition, bands ratio was similar among the all sections tested for a certain specimen, showing a good level of talc particle dispersion and distribution within the polymeric matrix (Fig. 3).

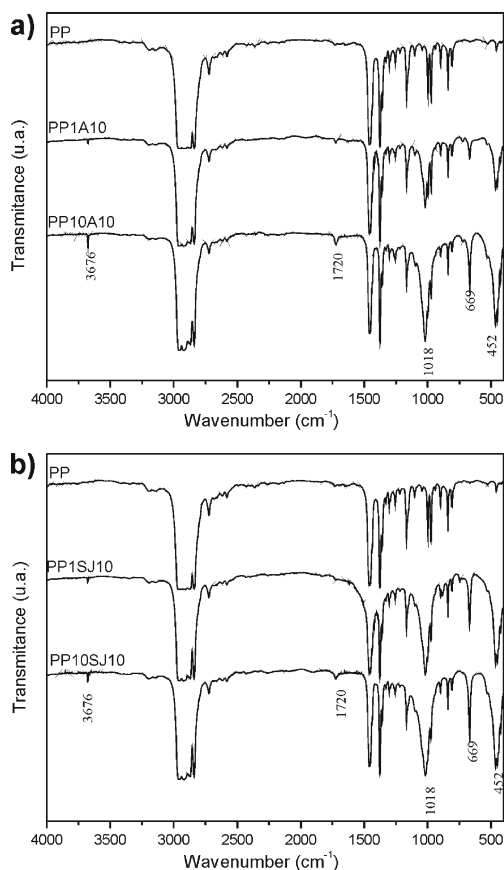


**Fig. 4** FTIR spectra of PP and **a** PP/A10 and **b** PP/SJ10 composites

## Composites crystalline morphology

Mechanical properties of particulate composites depend on matrix and filler intrinsic properties, concentration and interfacial adhesion as well as filler dispersion and distribution [9]. In addition, talc particles can induce changes in the crystalline structure of thermoplastic matrices (like PP), on account of their nucleating character. PP crystals might be modified in size, phase, perfection, quantity and orientation; which in turn will alter the composite mechanical performance [1]. In order to assess the incidence of talc morphology, PP crystallization was studied initially by dynamic thermal analysis followed by X-ray diffraction. Thermal study for both PP and composites was carried out at the same thermal history and cooling/heating rates. Figure 5 shows the crystallization curves of PP, PP/A10 and PP/SJ10 including their corresponding crystallinity degree ( $X_c\%$ ) values. A significant increment is observed in the crystallization temperature and  $X_c\%$  values for composites with 1 wt.% of talc, either for A10 and SJ10, compared to PP. This effect is attributed to the nucleating capability of talc as it was demonstrated by others authors [1]. Crystallization temperature for both sets of composites containing 1 wt.% of talc is around  $10\text{ }^\circ\text{C}$  higher than the corresponding to PP, being a clear evidence of the aforementioned fact. Concerning  $X_c\%$ , there is an increment up to 7 % when 1 wt.% of each talc is added to PP. Particularly, composites containing SJ10 talc show higher  $X_c\%$  than composites with A10 one. This behavior could be related to the talc morphology since large platelets of SJ10 promotes greater PP nucleation than the smaller ones corresponding to A10 talc [10]. Considering that crystalline induction takes place on active sites for nucleation on talc surface, and that both samples have similar particle size; a higher talc concentration should induce larger nucleating effect. However, this expected increment on  $X_c\%$  value is not observed, so a saturation effect of the nucleation sites appears to occur. Above certain talc concentration, the number of nucleation sites does not increase anymore and  $X_c\%$  becomes independent of talc morphology. These conclusions agree with previous results obtained either in our group studying the crystallization of PP/talc composites under isothermal conditions [11] or by others authors [12].

Predominant macrocrystalline talc induces higher crystallinity in PP than microcrystalline one, as was revealed by DSC experiments. However, this is not enough for a thorough characterization of PP crystalline phase in these composites. In order to distinguish possible differences between the induced crystalline structures by A10 and SJ10 talc, X-ray diffraction studies were performed on both sets of composites. Figure 6 presents the diffraction spectra of PP and PP/talc composites where the reflections corresponding to talc and PP are identified. The analysis is focused mainly on

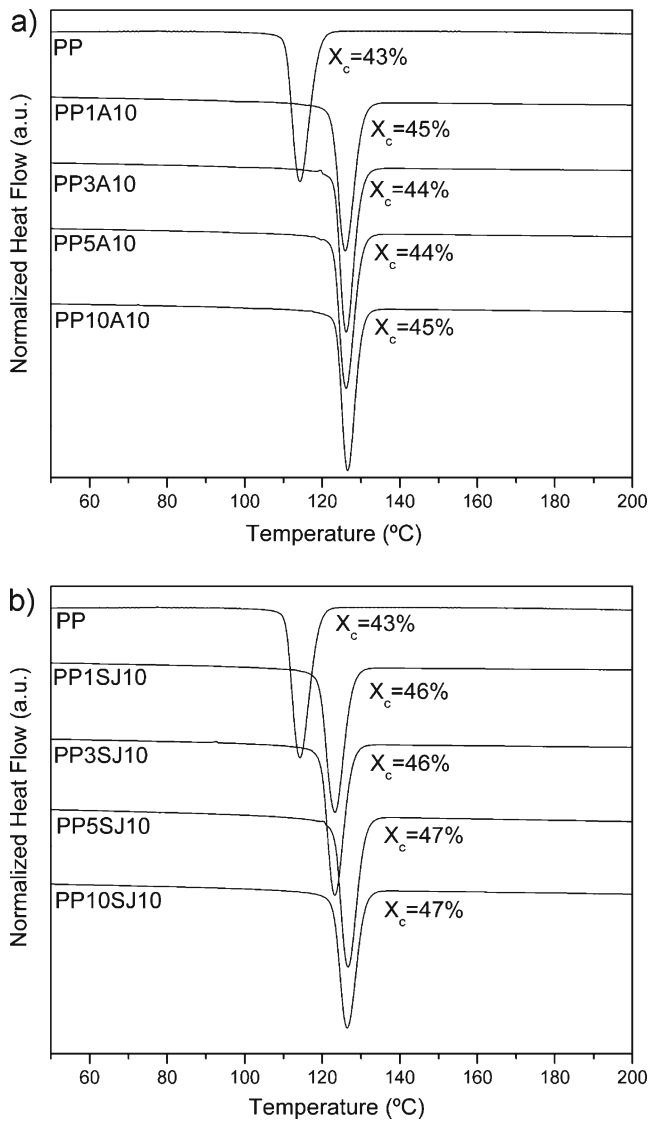


**Fig. 5** DSC crystallization thermograms with crystallinity degree for PP and **a** PP/A10 and **b** PP/SJ10 composites

the spectra from lowest talc content (1 wt.%) in order to avoid possible misleading effects due to particle-particle interactions. Particularly, when talc (either A10 or SJ10) is added to PP, a variation in the peak height of (110) and (040) planes of  $\alpha$ -phase from PP is observed. This variation can be used as indicator of the structural morphology induced by talc in PP. The nucleating efficiency of talc can be expressed as the intensity ratio between (040) and (110) reflections of  $\alpha$ -form [13]. Table 1 shows the intensity ratio of (040)/(110) reflections of PP and PP/talc composites. The ratio for PP differs from the reported in literature for isotropic structure (0.54) [14] due to injection molding favors the development of non-isotropic crystals [15]. Particularly, (040)/(110) values of PP1A10 and PP1SJ10 are similar, so the height of these reflections can be compared. The intensity of (040) reflection for PPSJ10 is 1.5 greater than for PP1A10, being

consistent with the notable growth of PP crystals on epitaxial direction observed for PP1SJ10 respect to PP1A10. This behavior is associated with the talc morphology. Considering the model proposed by Ferrage et al. [13] and the macrocrystallinity of SJ10, this talc has a larger surface available to the PP epitaxial growth. Talc particles are aligned parallel to the specimen surface having its  $c^*$  - axis perpendicular to the surface. On the other hand, PP crystallizes with a  $b^*$  - axis perpendicular to the specimen surface. So, talc  $c^*$  - axis merges with PP  $b^*$  - axis suggesting that  $b^*$  - axis of PP unit cell grows perpendicularly to the basal plane of talc particles due to the crystallographic plane similarities [16, 17].

A more detailed analysis from composites XRD spectra in the region  $2\theta=14-18^\circ$  reveals a significant difference between PP/A10 and PP/SJ10 composites. Figure 6 shows that for PP/SJ10 composites not only  $\alpha$  phase appears, but also  $\beta$  phase is present through (300) reflection. In this sense, it can be inferred that SJ10 talc induces and relatively rises  $\beta$  phase detected in PP. For 3 wt.% talc, the proportion

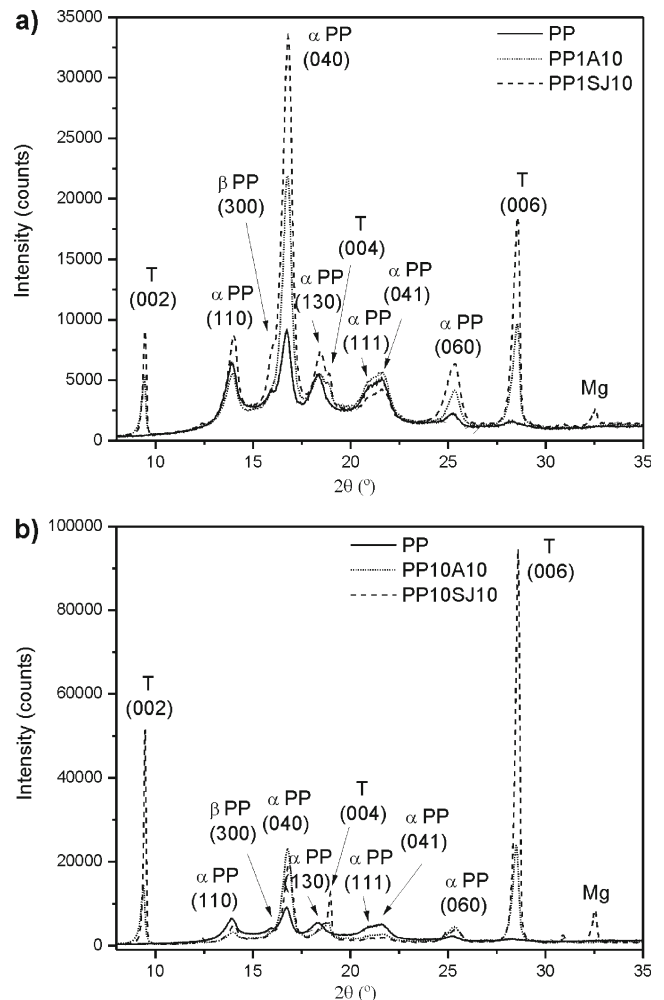


**Fig. 6** XRD spectra of PP, PP/A10 and PP/SJ10 composites with **a** 1 and **b** 10 wt.% talc

**Table 1** XRD intensity ratio [(040)/(110)] from PP and PP/talc composites spectra

Sample	(040)/(110)	Sample	(040)/(110)
PP	1.5		
PP1A10	4.7	PP1SJ10	4.2
PP3A10	6.8	PP3SJ10	2.4
PP5A10	8.4	PP5SJ10	4.2
PP10A10	8.5	PP10SJ10	4.2

of  $\beta$  phase is the largest one coinciding with the saturation concentration. Instead, in PP/A10 composites  $\beta$  phase disappears completely and it may be related to the talc morphology. A10 acts as an inhibitor of  $\beta$  phase, as reported in literature for microcrystalline talc [18, 19]. On the other hand, highly macrocrystalline talc induces  $\beta$  phase in composites. This phase has been reported to have higher values of elongation at break and strength than  $\alpha$  phase [20, 21]. As a consequence, the induced crystalline structure by macrocrystalline talc could bring a different mechanical performance in composite that later will be corroborated with mechanical properties measurements.

**Mechanical properties**

In order to assess the contribution of talc morphology on composite mechanical performance, tensile properties were determined for PP and PP/talc specimens and summarized in Table 2. Also, stress–strain curves were included in Fig. 7 to provide a better understanding on mechanical behavior of each composite set. Although the purity degree of talc samples is different, the comparison of final properties between two sets of composites is valid since the amount of associated minerals in both talc samples is less than 15 wt.%. In this case, talc nucleating character dominates

**Table 2** Mechanical properties of PP and PP/talc composites

Specimen/ Concentration (wt%)	E (MPa)	$\sigma_y$ (MPa)	$\epsilon_b$ (%)
PP	1623±13	33.4±0.2	214.5±7.2
PPA10			
1 %	1694±21	28.6±0.3	22.0±3.3
3 %	1793±18	28.2±0.3	22.1±3.1
5 %	1886±24	28.5±0.2	20.8±2.2
10 %	2041±24	28.1±0.3	18.8±2.2
PPSJ10			
1 %	1761±20	34.3±0.4	64.4±8.6
3 %	1871±8	34.2±0.2	52.8±12.0
5 %	1991±24	35.1±0.3	47.0±6.5
10 %	2332±20	35.1±0.3	43.9±10.5

over carbonates contribution on the enhancement of composite mechanical properties. The influence of talc platelets on PP crystallization is special, different from that occurring with other inorganic fillers even those of laminar morphology [22, 23]. The standard deviation of composite properties is relatively low (Table 2). This can be appreciated as an indication of good talc dispersion and distribution within matrix and, consequently, the presence of repetitive morphologies in the tested specimens as observed in SEM micrographs (Fig. 3).

Young modulus (E) of PP/talc composites containing both macro and microcrystalline talc samples were higher than pure PP. Particularly, modulus increment for 1 wt.% of talc, either for A10 or SJ10, seems to be a consequence of its nucleation ability since modulus cannot be strongly affected by additivity at this low concentration [24]. However, at higher talc concentration, the increment of modulus should

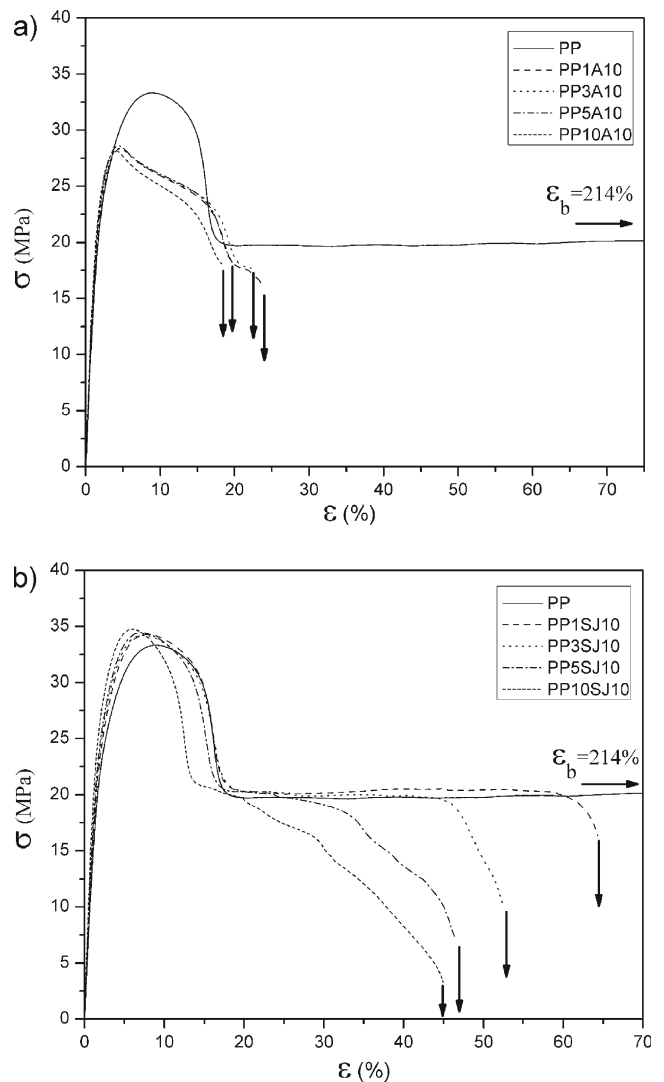
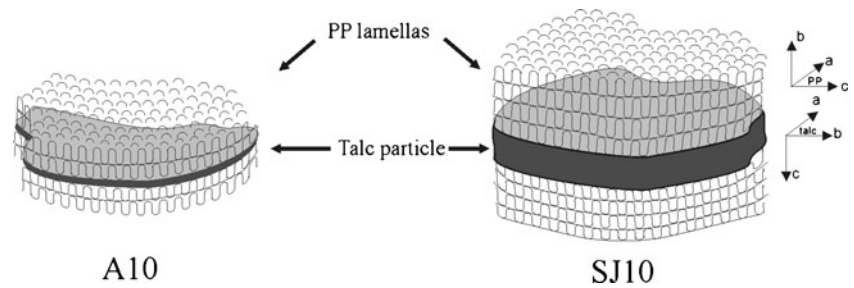


**Fig. 7** Stress–strain tensile curves for PP and a) PP/A10 and b) PP/SJ10 composites

**Fig. 8** Epitaxial PP crystal growth from A10 and SJ10 talc particle



arise from the contribution of talc stiffness ( $E_{\text{talc}} \approx 170$  GPa vs.  $E_{\text{PP}} \approx 1.7$  GPa), taking into account that  $X_c\%$  does not increase appreciably [25]. Other factor that may contribute to the composite modulus increment is the more uniform and smaller sized crystals resulting from talc addition, frequently associated to an increased stiffness [24]. Also, talc particle orientation, which depends on the processing method, plays an important role in the material stiffness [9]. In this work, all the specimens were injected by a high thickness film gate from one of its ends, assuring that the flow into the mold is plug like. During mold filling, talc/molten PP suspension flows and lamellar particles align straight along the flow direction (Fig. 3). However, PP/SJ10 composites show consistently higher modulus than PP/A10 ones and the variation can be as high as 14 % at 10 wt.% talc. This property difference might be explained in terms of talc morphology. As it was discussed above, particle lamellarity is closely related to morphology. In general, fillers with high aspect ratio (length/thickness ratio of filler particle) show a better stiffening effect than fillers with high particle symmetry [26]. In this sense, talc having a large aspect ratio (macrocrystalline) will give greater stiffness than microcrystalline talc at a given concentration [27].

The effect of macro and microcrystalline talc morphology on yield stress ( $\sigma_y$ ) is revealed by comparing the property values for PP/A10 and PP/SJ10. As it is known, tensile yield stress is a good indicator for interfacial interactions in heterogeneous polymer systems depending on the stress transfer trough

filler-matrix interphase [28]. Composites containing predominant microcrystalline talc (PP/A10) have lower  $\sigma_y$  values than PP, whereas composites with highly macrocrystalline one (PP/SJ10) show superior values than PP. At 10 wt.% talc, the decrement of  $\sigma_y$  for PP/A10 is 16 % and the increment for PP/SJ10 is 5 %, both respect to PP. This result can be interpreted considering the differences in filler-matrix interphase, depending on talc sample. The lower  $\sigma_y$  of PP/A10 composites respect to PP ones is probably due to the presence of small particles rounded by thin crystalline layer that favors A10 particles dewetting [9, 29, 30], decreasing  $\sigma_y$  and  $\epsilon_b$ , as discussed later. On the other hand, the increased  $\sigma_y$  values of PP/SJ10 composites respect to PP may be explained in terms of the induced crystal growth from talc surface. As it was seen before from XRD data, SJ10 talc favors the orientation of (040) PP crystals and it is clear the presence of a notable crystal population in this direction. This generates a thicker crystal epitaxial growth which allows supporting higher stress than A10 talc-PP interphase (Fig. 8).

Elongation at break ( $\epsilon_b$ ) of PP/A10 and PP/SJ10 composites seems to be the property more affected by talc morphology. It is observed in Fig. 7 that both composites show decreasing values with talc concentration. This behavior can be related to fillers that restrict matrix mobility, resulting in matrix reinforcement [31]. The  $\epsilon_b$  values for PP/SJ10 are higher than that PP/A10 ones suggesting that composites containing highly macrocrystalline talc have higher elongation at break than microcrystalline ones. This difference could be explained in terms of a more resistant PP-macrocrystalline talc interphase resulted from a more induced crystalline layer developed out of talc surface, allowing a larger specimen deformation up to breakage.

Mechanical performance of PP/A10 and PP/SJ10 agrees with the macroscopical behavior presented in the photographs of PP and both composite sets specimens after mechanical testing (Fig. 9). Typical characteristics of PP behavior as neck formation and a strong bleaching are observed on composites specimens [32]. All samples form neck, but its propagation differs between PP/A10 and PP/SJ10 composites. Composites containing predominant macrocrystalline talc show higher propagations than that microcrystalline talc agreeing with Fig. 7. This fact reveals a thicker crystal epitaxial growth developed from talc surface in PP/SJ10 composites. As a consequence, PP lamellas

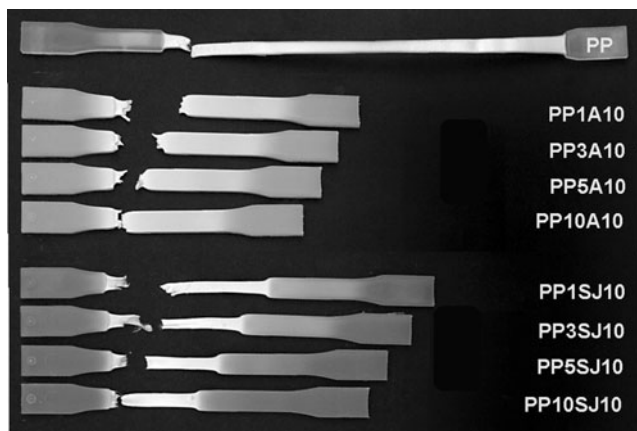


**Fig. 9** PP and PP/talc composites specimens after tensile test



allow a higher elongation when polymer chains start to extend during the neck formation.

## Conclusions

The effect of talc macro/microcrystalline morphology on mechanical properties of PP/talc composites is studied in this paper. Macro/microcrystallinity of talc samples which arise from different geological genesis were assessed through the corresponding morphology indexes. Two sets of composites prepared with these talc samples were compared. Composites were obtained by compounding in a twin screw extruder and molding by injection directly to dog bone shape specimens. The following conclusions can be drawn from this study:

- Highly macrocrystalline talc induces  $\beta$  phase in PP, increasing it respect to the detected one in pure PP. Meanwhile,  $\beta$  phase disappears completely in composites containing microcrystalline talc upon blending.
- Modulus of composites containing predominant macrocrystalline talc is consistently higher than the measured for microcrystalline ones. This modulus variation can be as high as about 14 % for 10 wt.% talc and it was explained in terms of talc lamellarity, intimately associated with morphology, being the main contribution to composite stiffness increment.
- Concerning elongation at break, a notable increase in necking propagation length was observed in tested specimens. Highly macrocrystalline talc shows a better interfacial interaction with PP than microcrystalline one and, consequently, it gives better composite toughness considering that no appreciable variation is detected in yield strength. This may be explained taking into account that macrocrystalline talc favors the orientation of (040) PP crystals, being clear the presence of a notable crystal population. This generates a thicker crystal epitaxial growth which allows supporting higher stress than microcrystalline talc-PP interphase.

The overall mechanical performance of composites is improved when predominant macrocrystalline talc is used. The properties are enhanced by both talc macrocrystallinity and induced crystalline morphology on PP.

## References

1. Pukánsky B (1995) In: Karger-Kocsis J (ed) Polypropylene. Structure, blends and composites. Chapman & Hall, UK
2. Piniakiewicz RJ, Mc Carty EF, Genco NA (1994) In: Carr DD (ed) Industrial minerals and rocks, 6th edn. SME Inc, Colorado
3. de Parseval P, Moine B, Fortuné JP, Ferret J (1993) In: Fenoll Hach-Ali P, Torres-Ruiz J, Gervilla F (eds) Current research in geology applied to ore deposits. University of Granada, Spain
4. Castillo L, Barbosa S, Maiza P, Capiati N (2011) *J Mater Sci* 46:2578–2586
5. Castillo L, Barbosa S, Capiati N (2013) *Polym Eng Sci* 53:89–95
6. Holland HJ, Murtagh MJ (2000) JCPDS-international centre for diffraction data 2000 advances in X-ray. *Analysis* 42:421–428
7. McCarthy EF, Genco N, Reade E Jr (2006) In: Kogel JE, Trivedi NC, Barker JM, Krukowski (eds) Industrial minerals and rock: commodities, markets and uses, 7th edn. Society for Mining, Metallurgy and Exploration Inc, USA
8. Rabello MS, White JR (1996) *Polym Compos* 17:691–704
9. Nielsen LE, Landel RF (1994) Mechanical properties of polymers and composites. Marcel Dekker Inc, New York
10. Gioffredi E (2012) Polymer crystallization: micro and nano filler effects on isotactic polypropylene. Ph.D. Thesis, Politecnico de Torino, Italy
11. Castillo L, Barbosa S, Capiati N (2012) *J Appl Polym Sci* 126:1763–1772
12. Rybnikar FJ (1989) *Appl Polym Sci* 38:1479–1490
13. Ferrage E, Martin F, Boudet A, Petit S, Fourty G, Jouffret F, Micoud P, de Parseval P, Salvi S, Bourgerette C, Ferret J, Saint-Gerard Y, Buratto S, Fortuné JP (2002) *J Mater Sci* 37:1561–1573
14. Addink EJ, Beintema J (1961) *Polymer* 2:185–193
15. Ferreira Custódio FJ (2009) Structure development and properties in advanced injection molding processes development of a versatile numerical tool. Ph.D. Thesis, Eindhoven, Technische Universiteit Eindhoven
16. Alonso M, Velasco JI, de Saja JA (1997) *Eur Polym J* 33:255–262
17. Fujiyama M, Wakino T (1991) *J Appl Polym Sci* 42:9–20
18. Pukánszky B, Belina K, Rockenbauer A, Maurer FH (1994) *Composites* 25:205–214
19. Zilhif AM, Ragosta G (1991) *Mater Lett* 11:368–372
20. Karger Kocsis J, Varga JJ (1996) *J Appl Polym Sci* 92:291–300
21. Tjong SC, Shen SJ, Li RK (1996) *Polymer* 37:2309–2316
22. Chen Z, Finet MC, Liddell K, Thompson DP, White JR (1992) *J Appl Sci* 46:1429–1437
23. Morales E, White JR (1988) *J Mater Sci* 23:3612–3622
24. Xavier SF (1991) In: Utracki LA (ed) Two-phase polymer systems. Hanser Publishers, Munich
25. Denac M, Musil V, Makarović M (1998) *Kovine Zlit Tehnol* 32:69–72
26. Chow TS (1978) *J Polym Sci: Polym Phys* 16:959–965
27. Clark RJ, Steen WP (2003) In: Karian H (ed) Handbook of polypropylene and polypropylene composites. Wiley, USA
28. Pukánszky B (1990) *Composites* 21:255–262
29. Fu S, Feng X, Lauke B, Mai Y (2008) *Composites: Part B* 39:933–961
30. van Dommelen J (2003) PhD Thesis Technische Universiteit Eindhoven
31. Echevarria GG, Eguiazabal JI, Nazabal J (1998) *Eur Polym J* 34:1213–1219
32. Song J, Prox M, Weber A, Ehrenstein GW (1995) In: Karger-Kocsis J (ed) Polypropylene: structure, blends and composites. Chapman & HaH, London